

# 1 Basic concepts

## 1.1 Introduction

Understanding the physical processes that determine the electrical resistivity of a concentrated metallic alloy is a daunting task because of the large number of possible contributions that could be involved. In addition to conduction electron scattering from thermally induced atomic displacements (which may depend upon concentration and degree of atomic and magnetic order) there will be other direct contributions from atomic and magnetic disorder, strain and band structure effects. The magnitude of such effects will be influenced by the homogeneity of the microstructure and will depend specifically upon whether the spatial extent or 'scale' of the inhomogeneity is greater or less than the conduction electron mean free path length.

The purpose of this first chapter is to introduce in a general way the relationship between the electrical resistivity and conduction electron scattering and band structure effects. It will be assumed that the reader is familiar with the fundamental concepts of electron waves in solids which have been very adequately considered in a variety of other texts (Ashcroft & Mermin 1976; Coles & Caplin 1976; Harrison 1970; Kittel 1976; Mott & Jones 1936; Blatt 1968; Ziman 1960, 1969, 1972). Other topics which are not specifically considered in detail in this text but which have been considered elsewhere include the electrical properties of pure metals (Meaden 1966; Wisner 1982; Pawlek & Rogalla 1966; Bass 1984; van Vucht *et al.* 1985), galvanomagnetic effects (Hurd 1974; Jan 1957), deviations from Matthiessen's rule (Bass 1972) and the electrical properties of intermetallic compounds (Gratz & Zuckermann 1982; Gratz 1983; Schreiner *et al.* 1982; Dugdale 1977, p. 279). A compilation of experimental data relating to the electrical resistivity of binary metallic alloys and rare-earth intermetallic compounds has recently been published by Schröder (1983).

## 1.2 Conduction electron scattering in solids

The electrical resistivity of a solid can be determined by passing a current  $i$  through the specimen of cross-section area  $a$  and measuring the resultant voltage drop  $v$  over a distance  $l$ . The electrical resistivity  $\rho$  is

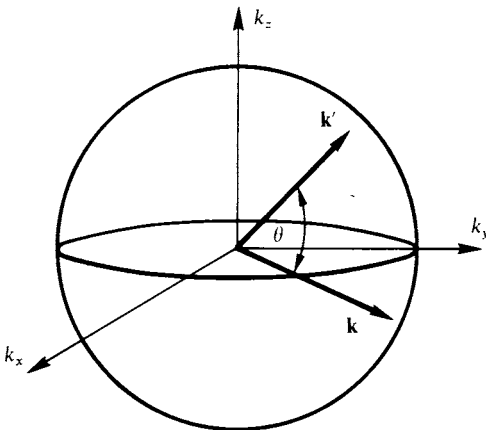
## 2 Basic concepts

then given by

$$\begin{aligned}\rho &= \frac{va}{il} \\ &= \frac{ra}{l},\end{aligned}\quad (1.1)$$

where  $r$  is the resistance of the specimen between the potential contacts. Despite the general acceptance of SI units, the resistivities of metals and alloys are usually given in units of  $\mu\Omega$  cm (units are discussed in more detail in Appendix A). Under the influence of an applied field the conduction electrons drift through an ionic array, the resistivity being determined by the rate at which they are scattered from some initial state  $\Phi_{\mathbf{k}}$  into a final state  $\Psi_{\mathbf{k}'}$ . This may be represented in  $\mathbf{k}$ -space as shown in Figure 1.1. As evident from the Fermi–Dirac distribution of electron energies (discussed later in relation to equation (1.23)), only electrons within an energy range  $\sim k_B T$  about the Fermi surface can increase their energy by some small amount under the influence of the external field. However, since the Fermi energy  $E_F \gg k_B T$  over the normal range of temperatures of interest, the vectors  $\mathbf{k}$  and  $\mathbf{k}'$  must terminate on the sharply defined Fermi surface. Note also that in the case of a spherical Fermi surface the maximum amplitude of the scattering wave vector is equal to  $2k_F$ . This scattering rate will be determined by the strength of the scattering potential  $V(\mathbf{r})$  and, in non-simple metals, the availability of states into which the electrons can be scattered. In terms of Fermi's

Fig. 1.1. Schematic representation of the scattering of a conduction electron from an initial state  $\mathbf{k}$  to a final state  $\mathbf{k}'$ .



'golden rule' the scattering probability can be written as

$$P_{\mathbf{k}\mathbf{k}'} = \frac{2\pi}{\hbar} |\langle \Psi_{\mathbf{k}'} | V(\mathbf{r}) | \Phi_{\mathbf{k}} \rangle|^2 N(E_F), \quad (1.2)$$

where  $\langle \Psi_{\mathbf{k}'} | V(\mathbf{r}) | \Phi_{\mathbf{k}} \rangle$  is the scattering amplitude for transitions between an initial state  $\Phi_{\mathbf{k}}$  and a final state  $\Psi_{\mathbf{k}'}$  (i.e. the matrix element of the scattering potential  $V(\mathbf{r})$  between the states  $\Phi_{\mathbf{k}}$  and  $\Psi_{\mathbf{k}'}$ ) and  $N(E_F)$  is the density of states at the Fermi energy  $E_F$  into which the electrons can be scattered. This latter term arises because of the necessity to have vacant states ready to accept the scattered electrons. Readers who may be unfamiliar with the notation in equation (1.2) should not despair. Examples will be given in the following chapters which show that many of the quantities required are available in the literature and that, in certain simplified cases, calculations can be performed on a programmable calculator or personal computer.

This scattering rate may be approximately described in terms of a relaxation time  $\tau$  averaged over the Fermi surface. In the simple case of a spherical Fermi surface (i.e. free conduction electrons)  $|\mathbf{k}'| = |\mathbf{k}| = k_F$  and the scattering probability  $P_{\mathbf{k}\mathbf{k}'}$  will depend only upon the angle  $\theta$  between  $\mathbf{k}$  and  $\mathbf{k}'$ . The relaxation time averaged over the Fermi surface can then be written as (see Chapter 5)

$$\frac{1}{\tau} \propto \int P(\theta)(1 - \cos \theta) dS$$

or

$$\frac{1}{\tau} \propto \int P(\theta)(1 - \cos \theta) \sin \theta d\theta, \quad (1.3)$$

where  $P(\theta)$  is now simply the probability of scattering through an angle  $\theta$  into the element of area  $dS$  on the Fermi surface and the integration variables are discussed in Appendix B. The term  $(1 - \cos \theta)$  essentially arises because we are only interested in the total change in momentum resolved in the direction of the electric field. For example, if we take the  $x$  direction to be in the direction of the applied field, the change in the contribution to the current from an electron will depend only upon the change in the  $x$  component of its velocity. Since the wavevector  $\mathbf{k}$  of a free electron will be in the same direction as its velocity, the change in the contribution to the current will be proportional to  $(k_x - k'_x)/k_x$ . (A more rigorous derivation will be given in Section 5.1.) The geometry of the problem in three dimensions is shown in Figure 1.2 and leads to the following relationships:

$$\left. \begin{aligned} k_x &= k_F \cos \alpha \\ k'_x &= k_F (\cos \alpha \cos \theta + \sin \alpha \sin \theta \cos \phi) \end{aligned} \right\} \quad (1.4)$$

## 4 Basic concepts

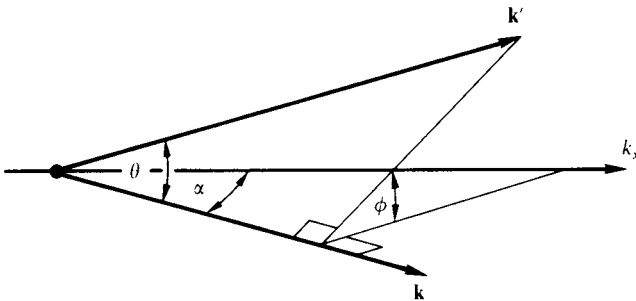
Averaging over  $\phi$  then gives the required result  $(k_x - k'_x)/k_x = 1 - \cos \theta$ . This term also has an important physical implication: it indicates that scattering through large angles is more important in determining the resistivity than small angle scattering. The significance of this fact will be emphasised in later chapters.

The final step in determining the resistivity is given by the Drude formula

$$\rho = \frac{m}{ne^2\tau}, \quad (1.5)$$

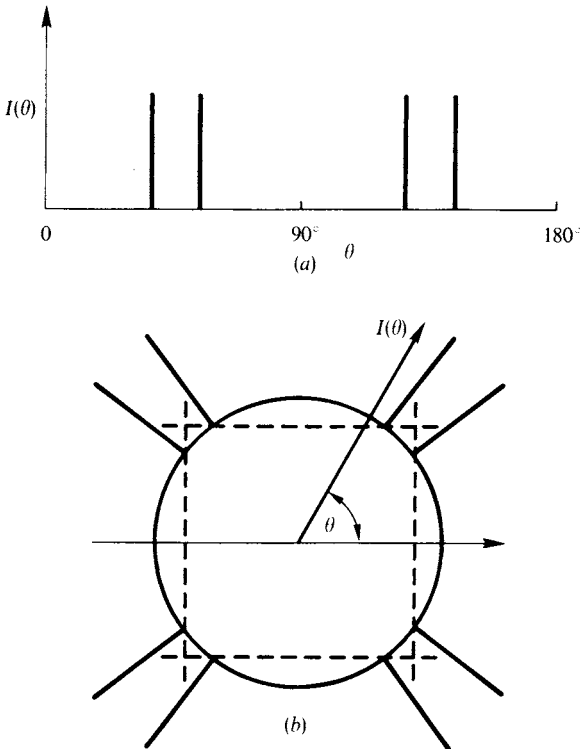
where  $n$  is the number per unit volume of electrons of mass  $m$  and charge  $e$ . It should be emphasised that this simple derivation has been given mainly to illustrate the link between the scattering process and the electrical resistivity. The assumptions of free electrons and a uniform scattering rate over a spherical Fermi surface are clearly severe restrictions on its applicability. One might expect them to be reasonable in the case of monovalent metals where the Fermi surface lies entirely within the first Brillouin zone, but generally the distortion of the Fermi surface and its intersection with the Brillouin zone boundaries might be expected to produce deviations from such simple behaviour in most metals or alloys. Nevertheless, in many concentrated alloys of interest (particularly those that do not contain transition metals) it appears that the Fermi surface is still roughly spherical, at least as far as the majority charge carriers are concerned, so that a 'nearly' free electron calculation can proceed. In other cases one clearly must take into account the effects of stronger scattering on the band structure of the alloy. These problems are discussed in more detail in relation to specific alloy systems in the chapters that follow. At this stage let us continue to use this simple model to illustrate some more features of the scattering process.

Fig. 1.2. Scattering geometry in three dimensions:  $\phi$  is the angle between the planes defined by  $\mathbf{k}$ ,  $\mathbf{k}'$  and  $\mathbf{k}$ ,  $x$  axis and  $\alpha$  is the angle between  $\mathbf{k}$  and the  $x$  axis.



The degree of periodicity of the ionic array determines the amount of electron scattering and hence the electrical resistivity. For example, in a perfectly periodic array (implying an infinite array of identical ions each at rest on a periodic lattice site) the electrons will suffer only Bragg scattering. (We treat here the general case where the electron wavelength is small enough to allow diffraction by the lattice, i.e. the Fermi surface intersects one or more Brillouin zone boundaries. If this is not the case there will be no Bragg scattering to worry about.) While the probability of scattering is then very large at the Bragg wavevectors, the scattering probability averaged over the Fermi surface is zero. This is because the Bragg scattering is very sharp and localised to a vanishingly small fraction of the Fermi surface, the width of the Bragg peaks being inversely proportional to the number of ions in the array,  $N$ . This behaviour is illustrated in Figure 1.3 which shows schematically the

Fig. 1.3. Bragg scattering: (a) in an ideal diffraction experiment and (b) superimposed on the Fermi surface. The Brillouin zone boundary is shown as a dashed line.

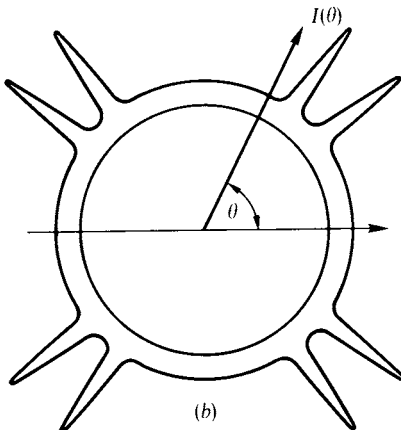
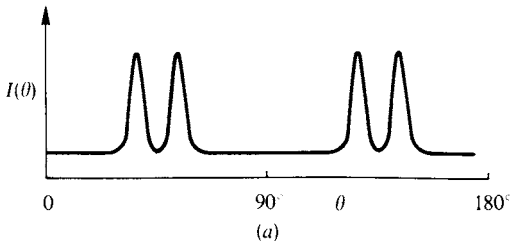


6 *Basic concepts*

Bragg scattering as it would be measured in a conventional diffraction experiment (corrected for all other sources of scattering and experimental broadening) and shows how such scattering would appear when plotted in a two-dimensional polar form in  $k$ -space. This form of plotting allows visualisation of the scattering superimposed on the Fermi surface.

The first Brillouin zone is also shown to emphasise the fact that Bragg diffraction occurs where the Fermi surface intersects the Brillouin zone boundary, this simply being a geometrical restatement of Bragg's law. In real solids the lack of perfect periodicity will give rise to additional diffuse scattering contributions, in direct analogy to the additional scattering (e.g. size or strain induced X-ray line broadening, short range order diffuse scattering and thermal diffuse scattering) observed in a diffraction experiment, as shown in Figure 1.4. This additional scattering will lead to a non-zero scattering probability when averaged over the Fermi surface and hence result in a finite value of the electrical resistivity.

Fig. 1.4. Schematic representation of scattering occurring in real materials showing the appearance of additional diffuse components.



### 1.3 Scattering anisotropy

Figure 1.4 also illustrates another important point. A purely random, free electron alloy would produce isotropic scattering with the scattering probability (and hence the relaxation time  $\tau$ ) having the same value at all points on the Fermi surface. However, as the deviation from randomness increases, the diffuse scattering will become unevenly distributed over the Fermi surface, leading to an anisotropic relaxation time  $\tau(\mathbf{k})$  that varies over the Fermi surface. Similar behaviour will result if the electron wavefunctions are not spherically symmetric since the electrons at different places on the non-spherical Fermi surface will have wavefunctions of different s-, p- and d-like character. Applying equation (1.3) would then lead to errors since it gives only an average reciprocal relaxation time  $\langle 1/\tau(\mathbf{k}) \rangle$  rather than properly taking into account the parallel contribution of all electrons to the total current flow. We return to this important problem later on. In the meantime it is important to note that an anisotropic relaxation time does not imply a direction dependence of the resistivity in real space. This is because the resistivity is determined from an average over all scattering directions (see, e.g. equation (1.3)) and will thus be isotropic in a cubic system in real space. In fact it is this very averaging process that makes interpretation of resistivity data so difficult. Unlike conventional diffraction techniques, which can map out scattered intensities in two- or three-dimensional reciprocal space, an electrical resistivity measurement gives only a single value at any particular temperature and state of disorder. As there is no means of performing the back-transform from this single point, analysis of resistivity data must rely on calculation of electron scattering based on some model of the structure or microstructure concerned.

### 1.4 Effects of the scale of microstructure

It is also important to consider the spatial extent or ‘scale’ of the atomic or magnetic correlations. This is because there is a characteristic conduction electron mean free path  $\Lambda$  defined by

$$\Lambda = v_F \tau, \quad (1.6)$$

where  $v_F$  is the velocity of the electron at the Fermi level. (Note that this suggests that  $\tau$  may be regarded as a ‘mean free time’.) This quantity is based on an average scattering probability and should not be simply interpreted as the real distance between scattering centres (see e.g. Sondheimer 1952). However, it may be taken as a measure of the coherence length of the electron wave. Within this context, the conduction electrons will only be scattered coherently by deviations from perfect periodicity which occur within a volume  $\sim \Lambda^3$ . This is because scattering centres separated by a distance greater than  $\Lambda$  do not

8 *Basic concepts*

produce coherent scattering, the electron having effectively ‘forgotten’ its phase once it has travelled a distance  $\sim \Lambda$ . This increases the complexity of the problem considerably: we need to consider deviations from perfect periodicity on a scale  $\Lambda$ , but  $\Lambda$  is in turn determined by electron scattering effects, and hence the degree of imperfection! While the ways around this problem will not be discussed until Chapter 5, such considerations do allow for the definition of ‘short’ and ‘long’ range atomic or magnetic correlations, depending upon whether their spatial extent (or correlation length) is less than or greater than  $\Lambda$  respectively. In fact this raises a point which is often overlooked. Whether a correlation is described as short or long range depends entirely upon the coherence length (or time) of the probe being used. For example, ‘long range order’ in a resistivity study typically implies strong correlations over volumes larger than  $1000 \text{ \AA}^3$ , whereas in a Mössbauer experiment ‘long range’ effects (e.g. quadrupole splitting) will result from correlations over much smaller distances, and may even be due to near neighbour effects representative of volumes of the order  $10 \text{ \AA}^3$ . In a dynamic problem such as spin fluctuation, similar considerations apply. For example, the lifetime of an excited state in a Mössbauer experiment (typically  $\sim 10^{-8}$  s) is very much longer than mean free time of a conduction electron (typically  $\sim 10^{-14}$  s) or a neutron ( $\sim 10^{-8}$ – $10^{-12}$  s). Thus, while spins in a material may appear to be strongly correlated (in time) in a Mössbauer experiment, a neutron diffraction or electrical resistivity study may lead to a quite different conclusion. Within the context of this book we will use the terms ‘short range’ and ‘long range’ as they apply to electrical resistivity studies, i.e. according to whether the correlation length is less than or greater than  $\Lambda$ , where  $\Lambda$  is typically  $\sim 10$ – $50 \text{ \AA}$  in concentrated binary alloys. These considerations are particularly important in the critical region since the atomic or magnetic correlation length is then rapidly changing with temperature and will pass from the short range to the long range regime as the temperature approaches the critical transition temperature from above. Problems associated with this behaviour are considered in Chapter 8.

One final point that relates to the significance of  $\Lambda$ : if a solid is so strongly disordered that the mean free path becomes comparable with the conduction electron wavelength ( $\sim 3$ – $4 \text{ \AA}$ ) then one might question the use of a diffraction model to determine the resistivity. This will occur when the residual resistivity reaches values over  $\sim 100 \mu\Omega \text{ cm}$ . However, a diffraction theory of the resistivity of liquid metals (Ziman 1969) produces results in reasonable agreement with experiment (even though the mean free path may be only roughly double the mean interatomic



spacing) and so there does seem to be some justification for its use. The particular problems associated with very high resistivity solid alloys and the adiabatic approximation are also considered in Chapter 8.

### 1.5 Matthiessen's rule

In the above discussion, no distinction has been made between disorder that is frozen into the lattice by quenching or equilibrium disorder, as would occur in an ordering alloy at high temperatures and at compositions away from stoichiometry, for example, and disorder that results from thermal excitation of the lattice. In dilute alloys (see Chapter 2) the scattering from impurity atoms is nearly independent of temperature and so the total resistivity  $\rho_{\text{tot}}(T)$  at any measuring temperature  $T$  can be written as the sum of two components

$$\rho_{\text{tot}}(T) = \rho_0 + \rho_{\text{h}}(T), \quad (1.7)$$

where  $\rho_0$  is the temperature independent residual (i.e. impurity) resistivity and  $\rho_{\text{h}}(T)$  is the resistivity of the pure host material at that temperature. This is known as Matthiessen's rule and will only be valid if the impurity and phonon scattering are independent and if the relaxation time is isotropic. These assumptions are only partly true in most systems and there is a large body of work devoted to studying 'deviations from Matthiessen's rule', DMR (see e.g. Bass 1972).

Matthiessen's rule is often applied to the case of concentrated alloys. This rather unfair extrapolation of Matthiessen's original work is then written as

$$\rho_{\text{tot}}(T) = \rho_0 + \rho_{\text{p}}(T) \quad (1.8)$$

and collects all contributions from scattering due to atomic disorder (excluding that due to thermally induced lattice displacements) into a residual resistivity  $\rho_0$ , leaving separate the phonon scattering of the alloy lattice  $\rho_{\text{p}}(T)$ . The first of these is usually described (with some confusion) as being 'temperature independent'. By this it is meant that, while  $\rho_0$  may of course depend indirectly upon temperature if the degree of atomic disorder changes with temperature, it does not have the *intrinsic* temperature dependence of  $\rho_{\text{p}}(T)$ . For example, an ordering alloy may be quenched to a temperature low enough to prevent atomic diffusion and a small change in measuring temperature  $T_{\text{m}}$  would then produce a change in  $\rho_{\text{p}}(T)$  but not  $\rho_0$ . Here one needs to be very careful about the specification of temperature and make a clear distinction between the measuring temperature  $T_{\text{m}}$  and the temperature that characterises the degree of disorder (the quench temperature  $T_{\text{q}}$ , for example). At measuring temperatures high enough to allow significant atomic diffusion, equilibrium may be attained, in which case these two

10 *Basic concepts*

temperatures will coincide. In magnetic alloys the dynamics of the spin system are usually such that the spins remain in thermal equilibrium down to very low temperatures, in which case it is more usual to express  $\rho_{\text{tot}}(T)$  as

$$\rho_{\text{tot}}(T) = \rho_0 + \rho_p(T) + \rho_m(T), \quad (1.9)$$

where  $\rho_m(T)$  is the temperature-dependent magnetic contribution resulting from spin-disorder.

However, in both the concentrated alloy and magnetic cases there are reasons to expect strong deviations from simple additivity. This is because the phonon spectrum is likely to depend upon both the concentration and degree of order, as are the electronic band structure and relaxation time anisotropy. Equations (1.8) and (1.9) should then properly include an additional term  $\Delta(T)$  to allow for these interactions. Nevertheless, it is often useful to identify the different contributions contained in an experimental result. Some aspects of this complicated problem are discussed in more detail in the following chapters.

### 1.6 Simple and non-simple metals

We move now to the definition of ‘simple’ and ‘non-simple’ metals. In order to make such a distinction we need to consider formally the ideas of electronic band structures, Fermi surfaces and density of states. In metals, all of these are determined by the valence or outer electron states. The band structure is obtained by solving the Schrödinger equation to obtain the energy as a function of wavenumber  $E(\mathbf{k})$  (see Chapter 4). The solutions are usually obtained along various

Fig. 1.5. Symmetry lines and points in the Brillouin zone for the fcc (a) and bcc (b) structures.

